2021 Fifth International Conference on Electrical, Electronics, Communication, Computer Technologies and Optimization Techniques (ICEECCOT) 10-11, December 2021

Underwater Image Enhancement using Scene-Specific Red Channel Prior and Fusion

Anparasy Sivaanpu
Department of Computer Science
University of Jaffna
Sri Lanka
anpusuji@gmail.com

Kokul Thanikasalam
Department of Physical Science
University of Vavuniya
Sri Lanka
kokul@vau.ac.lk

***Abstract*— Quality of underwater images are reduced with the depth since light is absorbed and scattered by the suspended particles in water. Although several optical model-based and model-free underwater image enhancement methods have been developed in the past, their performances are considerably poor since they fail to consider the scene-specific cues and depth information. In this study, a novel enhancement approach is proposed by combining optical model-based and model-free algorithms. In the model-based technique, a tentative depth map estimation technique is proposed and then used to compute more accurate red channel prior, background light, and transmission. White balancing and Gamma correction are used in the model-free technique. Outputs of both techniques have been combined by a fusion strategy to recover the details and colour. Experimental results demonstrate the proposed enhancement method outperforms state-of-the-art approaches on UIEB, OceanDark, and U45 benchmark datasets.**

Keywords—Underwater image enhancement, Red channel prior, Scene depth estimation, Depth map extraction

I. INTRODUCTION

Underwater images are often in poor quality since they have a reduced contrast, colour deviations, low brightness, and a foggy appearance. Therefore, extracting useful information from underwater images is a challenging task for many application areas such as marine species identification [1], underwater archaeology[2], control of submarines and other vehicles[3], and inspection of underwater infrastructures and cables[4]. Computer vision based enhancement techniques are used to restore the colour and details of underwater images without depending on expensive hardware based enhancement equipment.

Visibility of underwater images is poor since the light coming from underwater objects are scattered and absorbed by the suspended particles in water which causes low contrast images with a foggy appearance. In addition, since the red light has a longer wavelength than blue and green lights, it is absorbed more quickly than others. Due to this, green and blue lights reach further depths in underwater and hence produce a bluish or greenish effect in underwater images. Further, attenuation of underwater lights depends on the distance it travels and causes colour distortions in images. Since all these factors are depending on the depth of a scene from the surface of water, depth map estimation plays a major role in underwater image enhancement. However, depth map estimation of a single underwater image is not an easy task since a single image does not provide any depth information itself.

Over the past few years, many computer vision based approaches[5-10] have been developed to restore details in underwater images. These methods can be grouped as model-free approaches and model-based approaches based on the techniques they have used. Model-free approaches use simplified image processing techniques without considering the physical properties of light in underwater. These approaches use a wide range of linear and nonlinear enhancement algorithms such as colour correction and balancing[11, 12], Gamma correction[12], and Retinex[13]. Although model-free approaches are fast and recover more natural colours, since they fail to consider the spectral properties of underwater and the relation between depth and image degradation, their recovering performances are considerably low.

Model-based approaches analysis the atmospheric light propagation and transmission map in underwater and then use an atmospheric scattering model for image enhancement. Most of these approaches depend on prior knowledge and some observations to estimate the light attenuation and transmission map of underwater images. Based on the similarity of fog removal approaches[14, 15], several model-based techniques have been proposed such as Dark Channel Prior (DCP)[16-18], Red Channel Prior (RCP) [19], Blurriness Prior (BP) [20], and Underwater Dark Channel Prior (UDCP)[21, 22]. Model-based approaches are able to recover more details since they consider the light scattering physical information and then recover the image accordingly. However, model-based approaches are still struggling to find the accurate depth map from a single image. Therefore, in most situations, they recover the underwater images with unnatural colours.

Recently, a few approaches[5, 23, 24] are following the fusion technique in underwater image enhancement. These approaches generate two or more enhanced images using different algorithms and then fused them together to get a better result. In addition, another set of approaches[25, 26] used end-to-end machine learning techniques in underwater image enhancement. Since these approaches use Convolutional Neural Networks (CNN) with a huge number of parameters, they need a massive quantity of training data. To manage the data deficiency, they generate and use the synthetic images in training. Although these approaches showed significant improvement in underwater image enhancement, they consume more computational resources and therefore are not fit for real-time image enhancement.

Although model-free approaches produce more natural colours, their recovering performance is lower than model-based approaches. On the other side, model-based methods are still struggling to approximate the depth map of a single underwater image. Therefore, a considerable performance gap is observed in underwater image enhancement. To reduce this performance gap, we propose a novel framework for underwater image enhancement. We combine model-based and model-free algorithms to achieve better image recovering

978-1-6654-3272-6/21/$31.00 ©2021 IEEE

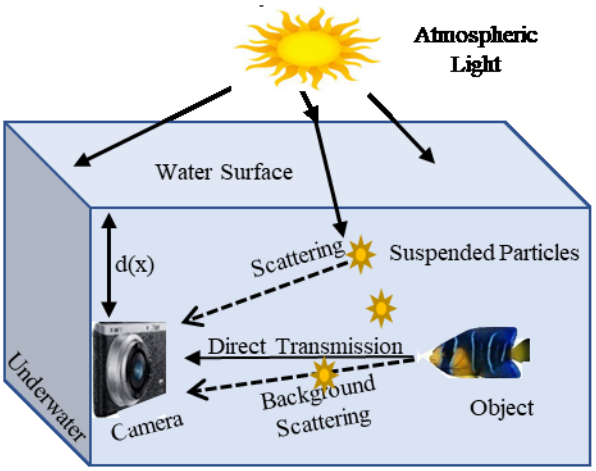

Fig.1: Underwater Image Formation Diagram

performance. In the proposed model-based technique, scene-specific depth map knowledge is obtained and then fed to measure the attenuation and transmission map. Then, a superpixel based segmentation technique is used to identify the equal depth regions in an underwater image. On the other side, white balancing and image sharpening algorithms are used in model-free technique. In the final stage of the proposed approach, both model-based and model-free techniques are fused to recover an underwater image with high contrast and natural colours. The performance of the proposed approach is measured on three well-known benchmark datasets and then compared with 14 model-based and model-free approaches. The proposed approach demonstrated excellent recovering performance in all three benchmarks.

II. Background

A. Underwater Image Formation Model

Quality of images are reduced in underwater by the attenuation differences of red, green, and blue lights as they can travel in water up to 5, 25, and 35 meters depth, respectively. Further, as shown in Fig.1, suspended underwater particles divert the track of light, which comes from the object. In underwater, direct transmission and background scattering lights are used to capture an object. The direct transmission is the light energy which directly came from the captured object. Background scatter is the light came from the object and then scattered by the suspended particles but still comes to the camera. These two components are used to form an image I as:

$$\mathrm{I(x)} = J^c(\mathrm{x})\, t^c(\mathrm{x}) + A^c\,(1 - t^c(\mathrm{x})), c \in \{r, g, b\}, \qquad (1)$$

where x represents a particular pixel in the captured underwater image, and $J^c(\mathrm{x})\, t^c(\mathrm{x})$ and $A^c\,(1 - t^c(\mathrm{x}))$ are the direct transmission and background scattering components, respectively. Also, in this equation, J^c is the non-degraded underwater image, t^c is the transmission medium coefficient, A^c is the background light in underwater, and $\{r, g, b\}$ are the red, green, and blue lights.

The transmission medium coefficient t^c describes the amount of light that is not affected by scattering or absorption and it can be written as:

$$t^c(\mathrm{x}) = \mathrm{e}^{-\beta^c \mathrm{d(x)}}, \qquad (2)$$

Where $\mathrm{d(x)}$ is the depth from the surface of the water and β^c is the attenuation coefficient for colour c. In this background, the model-based image enhancement approaches are objective to find the non-degraded image J, from the captured image I.

B. Red Channel Prior

In this study, the Red Channel Prior (RCP) [19] is used as the baseline model-based algorithm and hence reviewed in this section. Since RCP is fast and efficient, many researchers used it as the baseline algorithm for underwater image enhancement.

In underwater images, the red colour channel is absorbed more by water and hence loses intensity with depth, while the other two colours keep their intensities. Based on this fact, RCP algorithm calculates the red channel prior $\mathrm{J^{red}}$ of an underwater image as:

$$\mathrm{J^{red}} = \min_{\mathrm{y}\in\Omega(\mathrm{x})} \left(Min(1 - \mathrm{J^r(y)}), \mathrm{Min}(\mathrm{J^g}(y), \mathrm{Min}(\mathrm{J^b}(y)\right), \qquad (3)$$

where Ω (x) is a square shape local image patch centred at x. Based on the observation of many underwater images, $\mathrm{J^{red}}$ is low and tends to be zero in a non-degraded image J. This is called the Red Channel Prior. Depend on that observation, the transmission t^c is obtained as:

$$t^c(\mathrm{x}) = 1 - \min_{\mathrm{y}\in\Omega(\mathrm{x})} \left(\min_{\mathrm{c}} \frac{I^c(\mathrm{y})}{A^c}\right), \qquad (4)$$

RCP algorithm estimates the background light A^c by calculating the average of brightest red channel pixels. Based on the calculations of t^c and A^c, a non-degraded image J will be obtained from the captured image I.

The recovering performance of RCP and similar approaches are relying on the efficiency of red channel prior computation. These approaches use a fixed patch size (in Equation (3)) to compute the red channel and assume that the transmission is constant within a patch. We observed that the

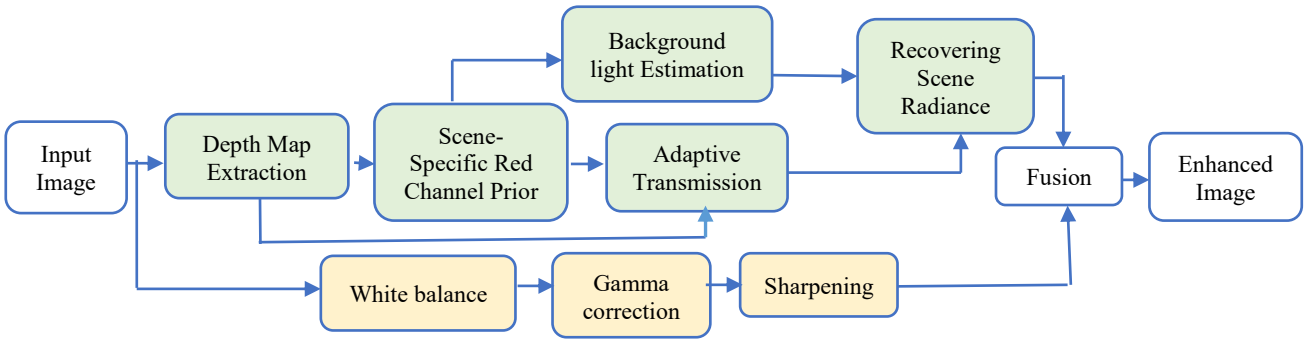

Fig. 2: Flow diagram of the proposed approach. An input degraded image is given to the model-based(green) and model-free(yellow) branches and then their outputs are fused together to obtain the enhanced image.

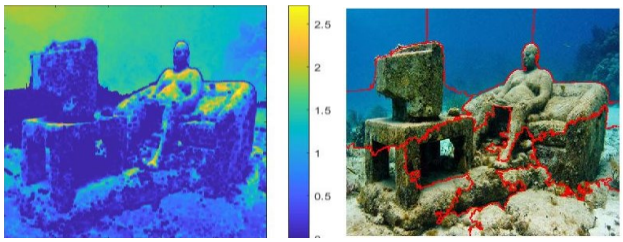

Fig. 3: Depth map extraction of an underwater image. (left) Intensity values of 1-I^r (right) Extracted equal depth map regions. Identified regions are shown in red.

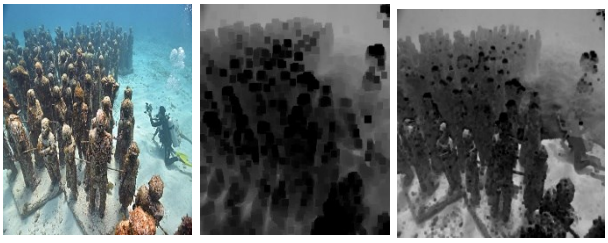

(a) (b) (c)

Fig. 4: Efficiency of the scene-specific red channel prior. (a) Input image. (b) Red channel prior in previous approaches. (c) Proposed scene-specific red channel prior.

enhancement performance is increased while the large patches are used in depth regions and small patches are used in less depth regions. Therefore, scene-specific patches should be used to increase the enhancement performance.

III. METHODOLOGY

The study objective to feed the depth map information to the red channel prior computation to improve the recovering capability of the model-based underwater enhancement approaches. In addition, this study focused on combining model-based and model-free techniques to obtain non-degraded images with natural colours. As shown in the Fig.2, the proposed methodology has two separate branches for model-based and model-free techniques. In the early phase of the proposed model-based technique, a tentative depth map is estimated and then utilised to compute the scene-specific red channel prior and transmission. On the other side, white balancing, image sharpening, and gamma correction algorithms are used in the model-free branch. Outputs of both branches are combined with a fusion technique. In the following subsections, each step is explained in detail.

A. Depth Map Extraction

Single image depth map extraction is one of the challenging and well-known problems in computer vision and machine learning. Although machine learning based algorithms are robust to predict the depth map, they are not suitable for a faster underwater image enhancement since they consume more computing resources and take too much time. In this scenario, a simple and faster depth map extraction technique is used in this study.

The proposed depth map extraction technique is built based on the observation that intensities of red colour channel pixel's intensities are inversely proportional to the depth of the water. This correlation can be written as:

$$I^r(x) \propto \frac{1}{d(x)}, I(x) = (I^r(x), I^g(x), I^b(x)), \qquad (5)$$

where $d(x)$ is the depth of the camera from the water surface and I is the captured image. As the initial step, a 3×3 patch is used to find the local minimum of red channel intensity values ($I^r(x)$). Then $1 - I^r(x)$ is calculated to forecast the tentative depth map of the image since it is proportional to the depth. Finally, equal depth map regions are identified using a superpixel based image segmentation technique[27]. As shown in Fig.3, proposed depth map extraction technique identifies the similar depth regions based on the intensity values of red channel intensity values.

B. Scene-Specific Red Channel Prior

Underwater image enhancement performance of RCP and other similar works are mainly relying on the computation of red channel prior. As stated in Equation 3, these approaches use a fixed size patch to find a lower intensity pixel and then that information is used to measure the transmission (Equation 4). However, based on our experiment, a large size of patch should be used in depth regions since probability for a lower intensity red channel pixel is low. Conversely, a small size of patch should be used in less depth regions since the probability for a lower intensity red channel pixel is high. Based on these findings, a scene-specific red channel prior computation is used in our method.

The extracted depth map regions are used to select the patch sizes in the proposed scene-specific red channel prior. As an initial step, average intensity of $1 - I^r(x)$ is computed for each similar depth region and then used to select the corresponding patch size. Since $1 - I^r(x)$ is proportional to the depth, large patch size is allocated for high average intensity of $1 - I^r(x)$. These details are summarized in Table1.

TABLE 1: PATCH SIZE ASSIGNMENTS BASED ON THE AVERAGE INTENSITIES

Average Intensity of $(1 - I^r(x))$	Patch Size (Ω)
$1 - I^r(x) \geq 230$	15 × 15
$230 > 1 - I^r(x) \geq 120$	11 × 11
$120 > 1 - I^r(x) \geq 80$	9 × 9
$1 - I^r(x) < 80$	5 × 5

After the patch size assignments, scene-specific red channel prior J_{R1}^{red} is calculated in a region $R1$ as follow:

$$J_{R1}^{red} = \min_{y \in \Omega'(x)} (Min(1 - J^r(y)), \text{Min}(J^g(y), \text{Min}(J^b(y)), \qquad (6)$$

where $\Omega'(x)$ is the patch size in region $R1$. Finally, the overall scene-specific red channel prior for an underwater image is calculated as:

$$J^{redS} = J_{R1}^{red} \cup J_{R2}^{red} \ldots . \cup J_{Rn}^{red}, \qquad (7)$$

where n is the amount of identified depth regions in the image and J^{redS} is the scene-specific red channel prior. As shown in Fig.4, more accurate results are produced by the proposed scene-specific red channel prior algorithm than the red channel prior in previous approaches.

C. Background Light Estimation

Similar to RCP and follow-up approaches, background light A^c, in an underwater image, is estimated by selecting the brightest pixel based on its scene-specific red channel prior.

D. Adaptive Transmission Estimation

Transmission (t^c) is the portion of the light that came from the scene to the camera without any scattering effect. As stated in Equation 4, transmission is calculated in RCP and follow-up approaches. However, in that calculation, we have

observed that unnatural colours are produced and the feeling of depth is lost while the entire scene-specific red channel prior (J^{redS}) is subtracted from 1. To avoid this, in the proposed approach, a very small amount of J^{redS} is kept in the transmission calculation by using an adaptive parameter ω (0< ω≤1). Based on that, the transmission calculation equation is modified as:

$$t^c(x) = 1 - \min_{y \in \Omega(x)} \left(\omega . \frac{1 - I^r(y)}{1 - A^r}, \frac{I^g(y)}{A^g}, \frac{I^b(y)}{A^b} \right), \quad (8)$$

where $A^c = (A^r, A^g, A^b)$ is the estimated background light. To produce more natural colours, small values of ω should be used in depth regions. Based on this concept, extracted equal depth map regions are used to assign the values for ω. Since intensities of $1 - I^r(y)$ are proportional to the depth of the scene, average intensities of $1 - I^r(y)$ are used to assign the values for ω. Table 2 shows the assignment of values for adaptive parameters ω based on the experimental results.

TABLE 2: ADAPTIVE PARAMETER ASSIGNMENT

Average Intensity of (1 – I^r(y))	Parameter (ω)
1 – I^r(y) ≥220	0.85
220 > 1 – I^r(y) ≥ 120	0.80
120 > 1 – I^r(y) ≥ 100	0.75
100 > 1 – I^r(y) ≥ 80	0.70
1 – I^r(y) < 80	0.65

E. Recovering Scene Radiance

In the final stage of the proposed model-based technique, non-degraded image J is recovered by using the background light A^c, and transmission t^c. The non-degraded image J is obtained as:

$$J^c(x) = \frac{I^c(x) - A^c}{Max(t^c(x), t_0)} + A^c, c \in \{r, g, b\} \quad (9)$$

Where t_0 is a parameter and set experimentally.

F. White Balance

In the proposed approach, a set of model-free image enhancement techniques are used to improve the colour of an underwater image. As an initial technique, a white balancing algorithm is used to remove the colour cast in underwater images. We have followed the white balancing technique of [12] without any modification. Based on that, enhanced red ($I^{r\prime}(x)$) and blue ($I^{b\prime}(x)$) colour channel intensities are calculated for a given input image $I(x)$ as:

$$\begin{aligned} I^{r\prime}(x) &= I^r(x) + \alpha . (\underline{I}^g - \underline{I}^r) . (1 - I^r(x) . I^g(x), \\ I^{b\prime}(x) &= I^b(x) + \alpha . (\underline{I}^g - \underline{I}^b) . (1 - I^b(x) . I^g(x), \end{aligned} \quad (10)$$

(a) (b) (c) (d)

Fig. 5: Illustration of the proposed fusion strategy. (a) Input image. (b) Output of model-based technique (c) Output of model-free technique (d) Fused image.

Where $\underline{I}^r$, $\underline{I}^g$, and $\underline{I}^b$ are the mean values of red, green, blue colours, respectively. α is a parameter and changed as per the illumination conditions.

G. Gamma Correction and Image Sharpening

Although, white balancing is used to recover the natural colours, it is not enough to recover the details near edges. Therefore, Gamma correction and image sharpening techniques are used in the next step of the proposed model-free technique. The intensity of the white balanced image is changed using the standard Gamma correction equation with Γ=2. In the final step of the model-free technique, edges of the image are sharpened by subtracting the input image from the blurred image.

H. Fusion Strategy

In the final stage of the proposed methodology, outputs of model-based and model-free techniques are fused to obtain a high-quality enhanced image. The following weight map is used to fuse the model-based (J_{mb}) and model-free (J_{mf}) outputs.

$$J_{Final} = \frac{J_{mb} + \delta J_{mf}}{1 + \delta}. \quad (11)$$

where J_{Final} is the fused output, and δ is a positive scalar and which is set experimentally. As shown in Fig.5, the proposed approach recover details from model-based technique (Fig.5(b)), and natural colours from model-free technique (Fig.5(c)). As shown in Fig.5(d), the proposed approach produces a better quality enhanced image by fusing model-based and model-free outputs.

IV. EXPERIMENTAL SETUP

A. Implementation details

In the proposed approach, all underwater and corresponding reference images are resized to 500 × 500. Matlab is used in the implementation. The values of t_0 (Equation 9) and δ (Equation 11) are set as 0.1 and 4, respectively. An Intel i7 processor is used to measure the performance of the proposed method. The results and code of this study are publicly available at (https://github.com/RPRO5/underwater_image_enhancement).

B. Datasets

Until recently, underwater image enhancement approaches are evaluated using synthetic images due to the unavailability of the benchmark datasets. However, in the last two years, three benchmark datasets are constructed and publicly available for the evaluation. Table 3 provides the information of these benchmark datasets.

TABLE 3: DETAILS OF THE BENCHMARK DATASETS

Details	Benchmark Datasets		
	UIEB[28]	OceanDark[29]	U45[30]
No. of images	890	183	45
Resolution	640 × 480	1280 × 720	256 × 256
Reference Image	Yes	No	No

Among these three datasets, UIEB has reference (non-degraded) images for each underwater images. Performance of the proposed approach is evaluated on these three benchmarks and then compared with the similar approaches.

TABLE 4: PERFORMANCE COMPARISON ON UIEB, OCEANDARK, AND U45 DATASETS

Approach	UIEB Dataset			OceanDark Dataset			U45 Dataset		
	PSNR ↑	MSE ↓	SSIM ↑	Entropy ↑	NIQE ↓	BRISQUE↓	Entropy ↑	NIQE ↓	BRISQUE ↓
Ours	**24.5543**	**1.1637**	**0.9206**	**8.1907**	**3.0222**	**20.2435**	**8.2947**	**3.5878**	**34.0426**
[19]	21.4763	3.3787	0.8891	7.5355	3.7833	23.8746	7.5381	5.0018	38.6867
[11]	15.9502	2.5637	0.8732	6.0495	4.2468	36.9381	7.3292	4.4804	38.0501
[24]	21.4468	2.8590	0.8706	7.6015	3.8876	23.8911	7.7370	4.8312	35.6663
[23]	22.6901	2.0411	0.8616	7.6179	3.4594	22.6629	7.7921	5.7651	36.8296
[31]	21.2501	4.7581	0.8604	7.5871	3.3804	30.2516	7.2964	4.2471	36.7397
[7]	20.4613	4.4734	0.8550	7.2249	3.9493	22.0136	6.8550	4.5387	37.9451
[6]	18.6016	3.6163	0.8505	5.2479	4.2074	41.9969	4.5171	4.4529	42.7003
[5]	20.3286	1.6820	0.8410	6.4201	5.2279	21.4155	7.6032	4.0253	35.3328
[13]	19.7149	2.7504	0.8314	7.6350	3.6506	32.7700	7.7409	4.5592	40.3740
[32]	18.5969	1.8117	0.8046	5.9159	3.6554	21.9463	5.8067	5.8540	35.8237
[12]	19.6032	1.8653	0.7601	7.2851	3.5770	24.9468	6.9338	4.9579	38.5485
[17]	13.6847	3.5327	0.7127	6.5501	3.8498	24.9626	7.0190	4.8598	37.3342
[8]	12.7935	4.2941	0.6537	6.8965	3.6826	26.4120	6.8069	5.0135	38.1648
[33]	13.5977	3.4435	0.5647	6.9267	3.9613	23.4299	6.8779	5.0051	38.1170

C. *Evaluation Criteria*

Generally, reference-based and non-reference based metrics are used to measure the performance of underwater image enhancement approaches. Reference-based metrics are used whenever non-degraded reference images are available. In this study, Structural Similarity Index (SSIM), Peak Signal-To-Noise Ratio (PSNR), and Mean-Squared Error (MSE) are used as the referenced-based metrics. A larger SSIM value represents that the output image is much similar to the reference image in terms of luminance, contrast, and structure. A higher PSNR and lower MSE represents that output image intensities are close to the reference image intensities for all three colour channels.

We have used Entropy, Blind/Referenceless Image Spatial Quality Evaluator (BRISQUE), and Natural Image Quality Evaluator (NIQE) the non-reference metrics. Entropy gives a high score for a high contrast and uniform image. NIQE is developed based on the human vision understanding of high-contrast areas of an image. A low NIQE score represents a better quality image. BRISQUE measures the naturalness in images and gives high scores for a worse image.

D. *Testing Results*

The enhancement performance of the proposed approach is evaluated on UIEB, OceanDark, and U45 benchmark datasets. We compared the performance with the model-free approaches of Fu et al.,[11], Sophiya and Gisha [24], Ancuti et al.,[23], Fu et al.,[13], Ghani et al.,[32], and Ancuti et al.,[12]. Further, we compared the model-based approaches of Galdran et al.,[19], Berman et al.,[31], Berman et al.,[7], Lee et al.,[6], Marques and Albu [5], Sathya et al.,[17], Yao and Xiang [8], and Chiang et al.,[33]. We obtained source codes of these approaches and evaluated their performances.

Table 4 Compares the enhancement of the proposed approach with other state-of-the-art approaches in UIEB, OceanDark, and U45 benchmark datasets. Based on the experimental results, our approach outperforms other approaches in all three benchmark datasets. Fig.6 shows the qualitative results of the proposed method with other four top-performing approaches. Based on that, it can be obviously seen that the proposed method recovers more details with natural colours.

TABLE 5: COMPARISON OF PROPOSED MODEL-BASED AND MODEL-FREE ALGORITHMS

Technique	PSNR	MSE	SSIM
Model-based	22.7658	1.6566	0.8473
Model-free	20.3384	2.6828	0.8979
Fused final output	**24.5543**	**1.1637**	**0.9206**

Since the proposed approach combines model-based and model-free algorithms, a comparison study is conducted to measure the individual performances of these algorithms. Their performances are evaluated on the UIEB dataset and

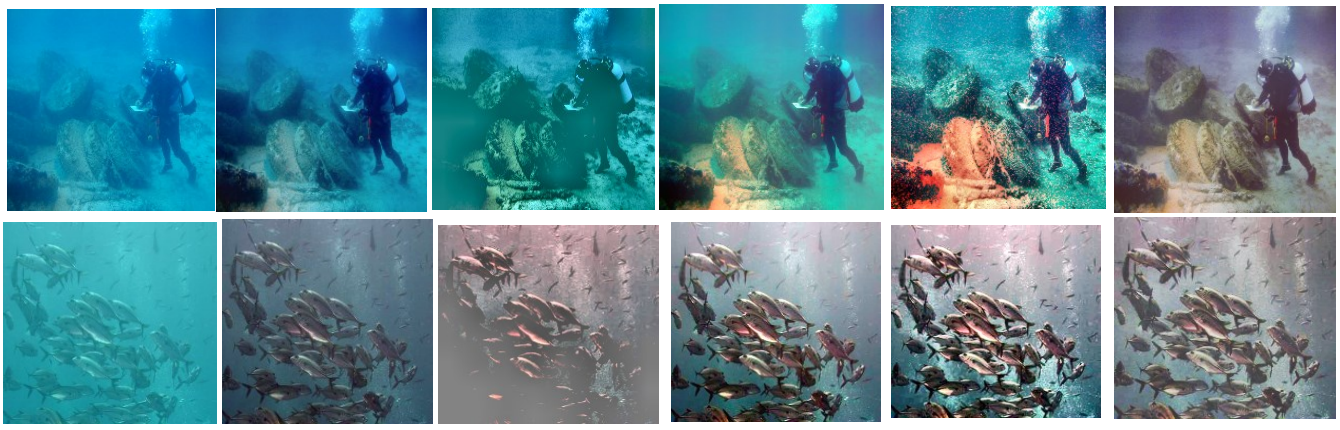

(a) (b) (c) (d) (e) (f)

Fig. 6: Qulaitative comparison with state-of-the-art approaches. (a) Input image (b) Galdran et al.,[21] 's result. (c) Fu et al.,[11]'s result, (d) Sophiya and Gisha [24]'s result, (e) Ancuti et al., [23]'s result, and (f) our result.

detailed in Table 5. Based on the results, it can be observed that the proposed model-based technique recovers an image with more details since it's PSNR is high and MSE is low. On the other hand, the proposed model-free technique contributes to recovering the colour and structure. In summary, fusion of proposed model-based and model-free techniques are used to recover an image with more details and natural colours.

V. CONCLUSION

In this study, we proposed a novel approach for single underwater image enhancement. Proposed approach has model-based and model-free branches of techniques to enhance the image. In the model-based technique, a tentative depth map of an underwater image is obtained based on the intensities of red channel pixels. In the next step, an image segmentation technique is used to identify the equal depth regions and then that information is fed to the estimation of red channel prior and transmission. In the model-free technique, white balancing and gamma correction are used to recover the natural colours of the image. Finally, a fusion strategy is used to combine the outputs of both techniques.

REFERENCES

[1] J. Ahn, S. Yasukawa, T. Sonoda, T. Ura, and K. Ishii, "Enhancement of deep-sea floor images obtained by an underwater vehicle and its evaluation by crab recognition," Journal of Marine Science Technology, vol. 22, pp. 758-770, 2017.

[2] F. Liarokapis, P. Kouřil, P. Agrafiotis, S. Demesticha, J. Chmelik, and D. Skarlatos, "3D modelling and mapping for virtual exploration of underwater archaeology assets," in International Workshop on 3D Virtual Reconstruction and Visualization of Complex Architectures, 2017.

[3] J. Guerrero, J. Torres, V. Creuze, and A. J. O. E. Chemori, "Adaptive disturbance observer for trajectory tracking control of underwater vehicles," Ocean Engineering, vol. 200, p. 107080, 2020.

[4] G. W. Thum, S. H. Tang, S. A. Ahmad, and M. Alrifaey, "Toward a Highly Accurate Classification of Underwater Cable Images via Deep Convolutional Neural Network," Journal of Marine Science Engineering vol. 8, pp. 924-945, 2020.

[5] T. P. Marques and A. B. Albu, "L2uwe: A framework for the efficient enhancement of low-light underwater images using local contrast and multi-scale fusion," in Proceedings of the IEEE/CVF Conference on Computer Vision and Pattern Recognition Workshops, pp. 538-539, 2020.

[6] H. S. Lee, S. W. Moon, and I. K. J. S. Eom, "Underwater image enhancement using successive color correction and Superpixel Dark Channel prior," Symmetry, vol. 12, p. 1220, 2020.

[7] D. Berman, D. Levy, S. Avidan, T. J. I. t. o. p. a. Treibitz, and m. intelligence, "Underwater single image color restoration using haze-lines and a new quantitative dataset," IEEE transactions on pattern analysis machine intelligence 2020.

[8] B. Yao and J. Xiang, "Underwater image dehazing using modified dark channel prior," in Chinese Control And Decision Conference (CCDC), pp. 5792-5797, 2018.

[9] W. Song, Y. Wang, D. Huang, and D. Tjondronegoro, "A rapid scene depth estimation model based on underwater light attenuation prior for underwater image restoration," in Pacific Rim Conference on Multimedia, pp. 678-688, 2018.

[10] S. Zhang, T. Wang, J. Dong, and H. J. N. Yu, "Underwater image enhancement via extended multi-scale Retinex," Neurocomputing, vol. 245, pp. 1-9, 2017.

[11] X. Fu, Z. Fan, M. Ling, Y. Huang, and X. Ding, "Two-step approach for single underwater image enhancement," in International Symposium on Intelligent Signal Processing and Communication Systems (ISPACS), pp. 789-794, 2017.

[12] C. O. Ancuti, C. Ancuti, C. De Vleeschouwer, and P. Bekaert, "Color balance and fusion for underwater image enhancement," IEEE Transactions on image processing, vol. 27, pp. 379-393, 2017.

[13] X. Fu, P. Zhuang, Y. Huang, Y. Liao, X.-P. Zhang, and X. Ding, "A retinex-based enhancing approach for single underwater image," in IEEE International Conference on Image Processing (ICIP), pp. 4572-4576, 2014.

[14] A. Sivaanpu and K. Thanikasalam, "Scene-Specific Dark Channel Prior for Single Image Fog Removal," International Journal on Advances in ICT for Emerging Regions, vol. 14, pp. 1-12, 2021.

[15] T. Kokul and S. Anparasy, "Single Image Defogging using Depth Estimation and Scene-Specific Dark Channel Prior," in 20th International Conference on Advances in ICT for Emerging Regions (ICTer), pp. 190-195, 2020.

[16] H.-Y. Yang, P.-Y. Chen, C.-C. Huang, Y.-Z. Zhuang, and Y.-H. Shiau, "Low complexity underwater image enhancement based on dark channel prior," in Second International Conference on Innovations in Bio-inspired Computing and Applications, pp. 17-20, 2011.

[17] R. Sathya, M. Bharathi, and G. Dhivyasri, "Underwater image enhancement by dark channel prior," in 2nd International Conference on Electronics and Communication Systems (ICECS), pp. 1119-1123, 2015.

[18] S. Serikawa, H. J. C. Lu, and E. Engineering, "Underwater image dehazing using joint trilateral filter," Computers Electrical Engineering, vol. 40, pp. 41-50, 2014.

[19] A. Galdran, D. Pardo, A. Picón, and A. Alvarez-Gila, "Automatic red-channel underwater image restoration," Journal of Visual Communication Image Representation, vol. 26, pp. 132-145, 2015.

[20] Y.-T. Peng, X. Zhao, and P. C. Cosman, "Single underwater image enhancement using depth estimation based on blurriness," in IEEE International Conference on Image Processing (ICIP), pp. 4952-4956, 2015.

[21] P. Drews, E. Nascimento, F. Moraes, S. Botelho, and M. Campos, "Transmission estimation in underwater single images," in Proceedings of the IEEE international conference on computer vision workshops, pp. 825-830, 2013.

[22] H. Wen, Y. Tian, T. Huang, and W. Gao, "Single underwater image enhancement with a new optical model," in IEEE International Symposium on Circuits and Systems (ISCAS), pp. 753-756, 2013.

[23] C. Ancuti, C. O. Ancuti, T. Haber, and P. Bekaert, "Enhancing underwater images and videos by fusion," in IEEE Conference on Computer Vision and Pattern Recognition, pp. 81-88, 2012.

[24] G. G. S. Sophiya Philip "Underwater Image Enhancement using White Balance and Fusion," International Journal of Engineering Research & Technology (IJERT), vol. 08, pp. 1-5, 2019.

[25] P. K. Sharma, I. Bisht, and A. Sur, "Wavelength-based Attributed Deep Neural Network for Underwater Image Restoration," arXiv preprint arXiv:.07910, 2021.

[26] X. Chen, P. Zhang, L. Quan, C. Yi, and C. Lu, "Underwater Image Enhancement based on Deep Learning and Image Formation Model," preprint arXiv:.00991, 2021.

[27] R. Achanta, A. Shaji, K. Smith, A. Lucchi, P. Fua, and S. Süsstrunk, "SLIC superpixels compared to state-of-the-art superpixel methods," IEEE transactions on pattern analysis machine intelligence, vol. 34, pp. 2274-2282, 2012.

[28] C. Li, C. Guo, W. Ren, R. Cong, J. Hou, S. Kwong, et al., "An underwater image enhancement benchmark dataset and beyond," IEEE Transactions on Image Processing, vol. 29, pp. 4376-4389, 2019.

[29] T. Porto Marques, A. Branzan Albu, and M. Hoeberechts, "A contrast-guided approach for the enhancement of low-lighting underwater images," Journal of Imaging, vol. 5, p. 79, 2019.

[30] H. Li, J. Li, and W. Wang, "A fusion adversarial underwater image enhancement network with a public test dataset," arXiv preprint arXiv:.06819, 2019.

[31] D. Berman, T. Treibitz, and S. Avidan, "Diving into haze-lines: Color restoration of underwater images," in Proc. British Machine Vision Conference (BMVC), 2017.

[32] A. S. A. Ghani and N. A. M. Isa, "Underwater image quality enhancement through Rayleigh-stretching and averaging image planes," International Journal of Naval Architecture Ocean Engineering vol. 6, pp. 840-866, 2014.

[33] J. Y. Chiang, Y.-C. Chen, and Y.-F. Chen, "Underwater image enhancement: using wavelength compensation and image dehazing (WCID)," in International Conference on Advanced Concepts for Intelligent Vision Systems, pp. 372-383, 2011.